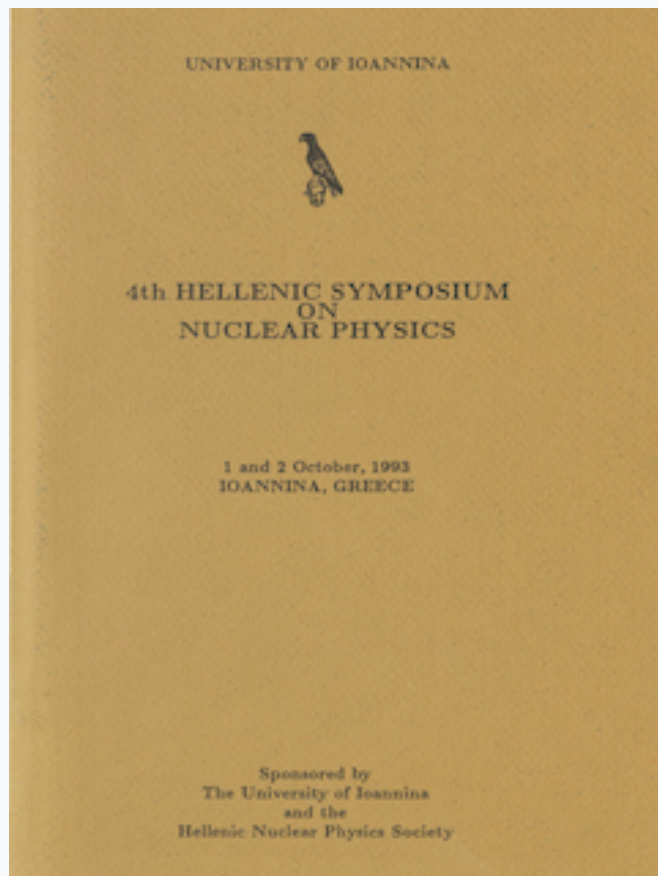


HNPS Advances in Nuclear Physics

Vol 4 (1993)

HNPS1993



The nucleon momentum distribution in light nuclei

K. N. Ypsilantis, M. E. Grypeos

doi: [10.12681/hnps.2878](https://doi.org/10.12681/hnps.2878)

To cite this article:

Ypsilantis, K. N., & Grypeos, M. E. (2020). The nucleon momentum distribution in light nuclei. *HNPS Advances in Nuclear Physics*, 4, 99–120. <https://doi.org/10.12681/hnps.2878>

THE NUCLEON MOMENTUM DISTRIBUTION IN LIGHT NUCLEI

K. N. Ypsilantis, M. E. Grypeos
Theoretical Physics Department
Aristotle University of Thessaloniki
GR-54006 Thessaloniki, Greece

Abstract

The nucleon momentum distribution in light nuclei is studied by means of a single particle potential model which consists of an attractive harmonic oscillator potential $V_a = \frac{1}{2}m\omega^2r^2$ and also of a repulsive one of the form $V_r = \frac{B}{r^2}$, $B > 0$. The latter simulates to some extend effects which would result if short range correlations were included (e.g. by a Jastrow factor) in a nuclear wave function, having as uncorrelated part a Slater determinant of harmonic oscillator orbitals. The main advantage of this model is that it leads to fairly simple analytic expressions for the momentum distribution of light nuclei and also for the density distributions and the elastic form factors. These expressions are quite useful in obtaining, for example, the asymptotic form of $\eta(k)$ for large k from which it is seen that the steep decrease of the nucleon momentum distribution observed with the harmonic oscillator model in this region is improved. Numerical results using various least squares fittings are obtained and discussed for a number of nuclei of the $1s, 1p$ shell.

1. Introduction

The nucleon momentum distribution $\eta(k)$ in nuclei is a quantity of particular interest in Nuclear Physics and has received considerable theoretical attention in the past and recent years. Ref. [1-5] are very useful reviews of this and of related subjects.

The nucleon momentum distribution contains information on the mean-field aspects of the nuclear many-body wave functions, and also on the effects of short-range nucleon-nucleon correlations which is complementary to that characterizing the density distribution in the r-space $\rho(r)$. For example $\eta(k)$ is much more sensitive to the finite size effects than $\rho(r)$. Thus, for ^{208}Pb , there is a factor of two between the calculated $\eta(k)$ at $k = 0$ and the nuclear matter value. On the other hand, the value of the density $\rho(r)$ at $r = 0$ is very close to the saturation value of nuclear matter [6]. We finally mention that both $\eta(k)$ and $\rho(r)$ can be related to measured quantities in electron scattering, though for the former much less experimental information is available in comparison to the latter.

Various theoretical approaches have been used for the calculation of the nucleon momentum distribution, which are appropriate for the study of light or medium and heavy nuclei and also nuclear matter (see for example refs. [3,6-23]). Many of these approaches are based on many-body techniques, which are usually quite complicated, in contrast to those using well-known single-particle models which are admittedly much simpler. However, the latter ones seem to lead to values of $\eta(k)$ which are unrealistically small in the region of large values of k . The agreement between the values obtained with many body approaches is not always sufficiently satisfactory but it is a characteristic feature of them to lead to larger values of the momentum distribution in the above mentioned region, compared to those obtained with the single particle models.

It is useful to recall that a single-particle wave function (Slater determinant) cannot reproduce simultaneously the charge form factor and the momentum distribution of a correlated system [19]. As our first results for 4He [24] indicate, however, one might be able to considerably improve the values of $\eta(k)$, calculated with an harmonic oscillator single particle wave function, in which the parameters have been fixed by fitting to the experimental charge form factor. This is achieved by suitably modifying the single particle potential.

The purpose of this paper is to use a modified harmonic oscillator potential, which contains a short-range repulsion and calculate the nucleon momentum distribution of light nuclei by determinig the parameters mainly by fitting of the calculated elastic charge form factor to the corresponding experimental values. The potential model is described in the next section where its advantages are pointed out. In the same section the density distribution and its m -th moment are given for nuclei of the $1s$ and $1p$ shell. In section 3, the analytic expressions for the form factor and the nucleon momentum distribution are given. In the final section the numerical results are presented and commented upon.

2. The single particle potential model, wave functions and density distributions.

The single particle potential which we assume for our treatment is

$$V(r) = -V_0 + \frac{1}{2}Kr^2 + \frac{B}{r^2} \quad (1)$$

where $V_0 > 0$, $B > 0$ and $K = m\omega^2 = \frac{\hbar^2}{m} \frac{1}{b^4} > 0$. This potential approaches the harmonic oscillator one at large distances r , but it has also a short range strong repulsion, an "infinite soft core", becoming infinite like r^{-2} as r tends to zero. The parameter K , or equivalently b , determines the "strength" of the attractive part while B the "strength" of the repulsive one. The equilibrium position r_0 for this potential may be calculated analytically and is given by

$$r_0 = \left(\frac{2B}{K} \right)^{1/4} = \left(\frac{2m}{\hbar^2} B \right)^{1/4} b \quad (2)$$

The main advantage in using potential (1) is that the Schrödinger eigenvalue problem can be solved analytically [25], not only for the ground state but also for any bound state. The energy eigenvalues are given by the simple expression

$$E_{nl} = -V_0 + \frac{\hbar}{2} \sqrt{\frac{K}{m}} \left[4n + 2 + \sqrt{(2l+1)^2 + \frac{8mB}{\hbar^2}} \right] =$$

$$= -V_0 + \frac{\hbar^2}{2m} \frac{1}{b^2} [4(n + \lambda_l) + 1] \quad n, l = 0, 1, 2, 3, \dots \quad (3)$$

where the parameter λ_l depends both on the orbital angular momentum quantum number and on the strength B of the repulsive part of the potential and is given by the expression

$$\lambda_l = \frac{1}{4} \left[1 + \sqrt{(2l + 1)^2 + \frac{8mB}{\hbar^2}} \right] \quad (4)$$

The normalized energy eigenfunctions are

$$y_{nlm}(r, \theta, \varphi) = R_{nl}(r) Y_l^m(\theta, \varphi) = \frac{\varphi_{nl}(r)}{r} Y_l^m(\theta, \varphi) \quad (5)$$

where the radial eigenfunctions φ are given analytically in terms of the confluent hypergeometric function

$$\varphi_{nl}(r) = \left[\frac{2\Gamma(n + 2\lambda_l + \frac{1}{2})}{n! [\Gamma(2\lambda_l + \frac{1}{2})]^2 b^{4\lambda_l + 1}} \right]^{1/2} r^{2\lambda_l} {}_1F_1(-n; 2\lambda_l + \frac{1}{2}; \frac{r^2}{b^2}) e^{-\frac{r^2}{2b^2}} \quad (6)$$

The $\varphi_{nl}(r)$ may be also expressed in terms of the associated Laguerre polynomials because of the relation of these polynomials to the confluent hypergeometric function [26]. The relevant expression is

$$\varphi_{nl}(r) = \left[\frac{2n!}{\Gamma(n + 2\lambda_l + \frac{1}{2}) b^{4\lambda_l + 1}} \right]^{1/2} r^{2\lambda_l} L_n^{2\lambda_l - \frac{1}{2}} \left(\frac{r^2}{b^2} \right) e^{-\frac{r^2}{2b^2}} \quad (7)$$

It may be easily checked that when $B = 0$, that is when $\lambda_l = \frac{1}{2}(l + 1)$, the above expressions coincide with the well known expressions for the radial harmonic oscillator eigenfunctions. It is also immediately seen that the wave functions for the ground state and the first excited ones are given by very simple expressions, as in the case of the harmonic oscillator potential.

Knowing the eigenfunctions, the (normalized to unity) point-proton density distributions of closed shell nuclei may be calculated by using the expression

$$\rho(r) = \frac{1}{4\pi Z} \sum_{nl} 2(2l + 1) R_{nl}^2(r) \quad (8)$$

In the case of open shell-nuclei we may use as an approximation the "average radial density" defined by

$$\rho(r) = \frac{1}{4\pi} \int \rho(\vec{r}) d\Omega \quad (9)$$

Thus, the expression used for $\rho(r)$ is

$$\rho(r) = \frac{1}{4\pi Z} \sum_{nl} \eta_{nl} R_{nl}^2(r) \quad (10)$$

where the summation is over the quantum numbers n and l of occupied proton states and η is the number of protons occupying the states with given n and l . Obviously, for the closed shell nuclei $\eta_{nl} = 2(2l+1)$. Quite analogous is the expression of the (normalized to unity) point-neutron density. Since we are interested in light nuclei with $N = Z$, the same expressions may be used as an approximation of the corresponding point-nucleon or "body" density distribution $\rho_B(r)$. As we mentioned in the introduction we focus our attention on the $1s$ and $1p$ nuclei.

The interesting feature of the single particle model we are using is that the following simple expression for $\rho(r)$ arises for nuclei with 2 protons in the $1s$ shell and $Z - 2$ protons in the $1p$ shell:

$$\rho(r) = \frac{1}{Z} \left[\frac{1}{\pi b^3 \Gamma(2\lambda_0 + \frac{1}{2})} \frac{r^{4\lambda_0-2}}{b^{4\lambda_0-2}} e^{-\frac{r^2}{b^2}} + \frac{Z-2}{2} \frac{1}{\pi b^3 \Gamma(2\lambda_1 + \frac{1}{2})} \frac{r^{4\lambda_1-2}}{b^{4\lambda_1-2}} e^{-\frac{r^2}{b^2}} \right] \quad (11)$$

This is a little more complex than the corresponding harmonic oscillator expression and coincides with it for $\lambda_l = \frac{1}{2}(l+1)$, $l = 0, 1$ [27].

It should be noted that the above expression can be easily generalized to allow for state dependence of the potential parameters. In such a case we have

$$\rho(r) = \frac{1}{Z} \left[\frac{1}{\pi b_0^3 \Gamma(2\lambda_0 + \frac{1}{2})} \frac{r^{4\lambda_0-2}}{b_0^{4\lambda_0-2}} e^{-\frac{r^2}{b_0^2}} + \frac{Z-2}{2} \frac{1}{\pi b_1^3 \Gamma(2\lambda_1 + \frac{1}{2})} \frac{r^{4\lambda_1-2}}{b_1^{4\lambda_1-2}} e^{-\frac{r^2}{b_1^2}} \right] \quad (12)$$

It should be understood that now λ_0 and λ_1 differ not only because of the different value of l ($l = 0$ and $l = 1$, respectively), but also because of the different value of B .

We may also note that the m -th moment $\langle r^m \rangle$ of the density distribution ρ may be calculated analytically. The result is

$$\langle r^m \rangle = \frac{2}{Z} \left[b_0^m \frac{\Gamma(\frac{4\lambda_0+m+1}{2})}{\Gamma(2\lambda_0 + \frac{1}{2})} + \frac{Z-2}{2} b_1^m \frac{\Gamma(\frac{4\lambda_1+m+1}{2})}{\Gamma(2\lambda_1 + \frac{1}{2})} \right] \quad (13)$$

Among the various moments the "mean-square radius" of the density distribution is given simply by

$$\langle r^2 \rangle = \frac{2}{Z} [b_0^2 (2\lambda_0 + \frac{1}{2}) + \frac{Z-2}{2} b_1^2 (2\lambda_1 + \frac{1}{2})] \quad (14)$$

Again these expressions coincide with the corresponding harmonic oscillator ones for $\lambda_l = \frac{1}{2}(l+1)$. It is seen from (14) that when the potential becomes less attractive, that is when b and λ increase, the mean square radius increases, as one should expect.

3. The analytic expressions for the elastic form factors and the momentum distributions

The point-proton elastic form factor in Born approximation may be obtained analytically by performing the Fourier transform of the corresponding density distribution (12):

$$F(q) = \frac{2}{Z} \left[{}_1F_1(1-2\lambda_0; \frac{3}{2}; \frac{b_0^2 q^2}{4}) e^{\frac{-b_0^2 q^2}{4}} + \frac{Z-2}{2} {}_1F_1(1-2\lambda_1; \frac{3}{2}; \frac{b_1^2 q^2}{4}) e^{\frac{-b_1^2 q^2}{4}} \right] \quad (15)$$

In this section too, we consider nuclei with two protons in the $1s$ shell and $Z-2$ protons in the $1p$ shell and we allow also for different potential parameters in each of these shells.

The elastic charge form factor $F_{ch}(q)$ can be calculated by performing the Darwin-Foldy correction $f_{DF}(q)$, the finite proton size correction $f_p(q)$ and the correction for the center of mass motion. By performing the latter, one obtains an expression $\tilde{F}(q)$ from $F(q)$. Unfortunately, as it is well known, this can not be done in a unique and exact way for a single-particle potential, except for the harmonic oscillator one in which case a Tassie and Barker correction factor [28] $\exp(\frac{b^2 q^2}{4A})$ arises: $\tilde{F}(q) = \exp(\frac{b^2 q^2}{4A}) F(q)$. Use of such a factor, even in an approximate way, does not seem to be generally appropriate in our case. The best thing which seems that one can do is to

use the "fixed centre of mass correction" [29] which for 2He leads to the expression

$$\tilde{F}(q) = \frac{\int d^3\omega F(|\vec{q} + \vec{\omega}|)F^3(\omega)}{\int d^3\omega F^4(\omega)} \quad (16)$$

The integrations in the above expressions are carried out numerically in our case, which is not so convenient and it is also expected to lead to inaccuracies, in particular at large values of momentum transfers. They are feasible, however, and we have in fact used expression (16) in reporting our first results for 2He [24]. For heavier nuclei, it is impracticable to use such a procedure in our approach. In view of this, we resort to using simply the reduced nucleon mass in the form factor $F(q)$, although such a treatment is ambiguous. For 2He , however, a comparison with the results obtained with the fixed center of mass correction, shows that the quality of the fit, though less satisfactory, does not change too much in this case (see next section). We also note that for the results we obtained for $F_{ch}(q)$ with the harmonic oscillator model and we display also in the next section, the usual Tassie and Barker correction was used.

Concerning the correction for the finite proton size, the Chandra and Sauer [30] proton charge form factor

$$f_p(q) = \sum_{i=1}^3 A_{p_i} e^{-\frac{a_{p_i}^2 q^2}{4}} \quad (17)$$

where

$$A_{p_1} = .506373, A_{p_2} = .327922, A_{p_3} = .165705$$

$$a_{p_1}^2 = .431566 fm, a_{p_2}^2 = .139140 fm, a_{p_3}^2 = 1.52554 fm$$

was used. Other similar expressions [31] may also be used.

The expression of the charge form factor which is therefore used in fitting the experimental results for the $1s, 1p$ nuclei is:

$$F_{ch}(q) = f_{DF}(q)f_p(q)\tilde{F}(q) =$$

$$= \frac{2}{Z} \sum_{i=1}^3 A_{p_i} \left[{}_1F_1(1 - 2\lambda_0; \frac{3}{2}; \frac{b_0^2 q^2}{4}) e^{-\frac{c_{p_i}^2 q^2}{4}} + \frac{Z-2}{2} {}_1F_1(1 - 2\lambda_1; \frac{3}{2}; \frac{b_1^2 q^2}{4}) e^{-\frac{c_{p_i}^2 q^2}{4}} \right] \quad (18)$$

where

$$c_{0i}^2 = a_{pi}^2 + b_0^2 + \frac{1}{2m^2}, \quad c_{1i}^2 = a_{pi}^2 + b_1^2 + \frac{1}{2m^2}$$

From expression (18) we can find the number of zeros of the form factor in the case of 4He . It is well known that the confluent hypergeometric and the Whittaker's function are related as follows

$${}_1F_1\left(\frac{1+a}{2} + k; 1+a; -z\right) = e^{-\frac{z}{2}} z^{-\frac{1+a}{2}} M_{k, \frac{a}{2}}(z)$$

where M is the Whittaker's function. The number of zeros of the function ${}_1F_1$ is the number of zeros of the function

$$f(k, a, z) = z^{-\frac{1+a}{2}} M_{k, \frac{a}{2}}(z)$$

which is known [32]

$$N = \begin{cases} 0 & \text{for } -\infty < k < \frac{1+a}{2} \\ -[\frac{1+a}{2} - k] & \text{for } \frac{1+a}{2} \leq k < +\infty \end{cases}$$

In our case

$$N = \begin{cases} 0 & \text{for } -\infty < \lambda_0 < \frac{1}{2} \\ -[1 - 2\lambda_0] & \text{for } \frac{1}{2} \leq \lambda_0 < +\infty \end{cases} \quad (19)$$

where $[x]$ is the maximum integer which is smaller than (or equal to) x . Thus we have the following table:

Values of λ_0	0	1/2	1	3/2	2	5/2	...
Number of zeros of $F(q)$	0	1	2	3	4	...	

By using the above table we can obtain the number of diffraction minima and compare with the known experimental data. The value of λ_0 which is found from the various fittings is on the average ~ 0.7 . It is seen from the above table that the charge form factor for 4He has one diffraction minimum. The existing experimental data have also one diffraction minimum.

Another rather interesting feature regarding the form factor of 4He in the framework of the present approach is that the position of the diffraction minima may also be given analytically in an approximate way. This may be done by noting [26] that the n -th root of the confluent hypergeometric function is given by the expression

$$x_n \simeq \frac{j_{c-1,n}^2}{2c - 4a} \quad (20)$$

where

$$j_{c-1,n} \simeq \pi \left(n + \frac{c}{2} - \frac{3}{4} \right) \quad (21)$$

is the n -th positive root of the Bessel functions $J_{c-1}(x)$. Thus we may write for the approximate value of the q^2 where the diffraction minima appear

$$q_n^2 \simeq \frac{4\pi^2 n^2}{b^2(8\lambda_0 - 1)}, \quad n = 1, 2, 3, \dots \quad (22)$$

It is seen, on the basis of the above analysis, that the number of the diffraction minima of the charge form factor of 4He depend on λ_0 that is on the strength of the repulsive part of the potential, while their position depends both, on λ_0 and b that is on the strength of the repulsive and of the attractive part. The stronger the repulsive part the larger the number of the diffraction minima. In addition, the position of each diffraction minimum is moved to smaller values of momentum transfer when the attractive part becomes weaker (b increases) and also when the repulsive part becomes stronger (λ increases).

It is obvious that the above results hold also for the charge form factor of 4He since the proton form factor $f_p(q)$ has no roots. It does not seem, however, possible to extend the above analysis to heavier nuclei.

We also note that by Fourier transforming of (18) we may obtain an analytic expression for the charge density distribution and its m -th moment. These expressions are, however, quite complex, the former one containing also Hermite polynomials. It is therefore preferable in practice to use numerical integration. Nevertheless, the mean-square radius is given, by a fairly simple analytic expression, namely

$$\langle r^2 \rangle_{ch} = \frac{3}{Z} \sum_{i=1}^3 A_{pi} \left[c_{0i}^2 + \frac{Z-2}{2} c_{1i}^2 - \frac{2}{3} \left[(1-2\lambda_0)b_0^2 + \frac{Z-2}{2} (1-2\lambda_1)b_1^2 \right] \right] \quad (23)$$

Regarding the nucleon momentum distributions, these may be obtained by means of the wave functions $\tilde{y}_j(k)$ in momentum space

$$\tilde{y}_j(\vec{k}) = \int y_j(\vec{r}) e^{i\vec{k}\vec{r}} d\vec{r} \quad (24)$$

through the formula [3]

$$\eta(\vec{k}) = \sum_{j=1}^A |\tilde{y}_j(\vec{k})|^2 \quad (25)$$

where A is the mass number. In the case of $1s$, $1p$ nuclei this leads after some algebra to the following expression:

$$\begin{aligned} \eta_{sp}(k) = & \frac{\pi 2^{2\lambda_0+2} (2b_0)^3 \Gamma^2(\lambda_0 + 1)}{\Gamma(2\lambda_0 + \frac{1}{2})} e^{-b_0^2 k^2} {}_1F_1^2(\frac{1}{2} - \lambda_0; \frac{3}{2}; \frac{b_0^2 k^2}{2}) + \\ & + (A-4) \frac{\pi 2^{2\lambda_1+1} (2b_1)^3 (kb_1)^2 \Gamma^2(\lambda_1 + \frac{3}{2})}{9\Gamma(2\lambda_1 + \frac{1}{2})} e^{-b_1^2 k^2} {}_1F_1^2(1 - \lambda_1; \frac{5}{2}; \frac{b_1^2 k^2}{2}) \end{aligned} \quad (26)$$

This expression is derived from another one, in which two confluent hypergeometric functions appear in the second term, which however, may be reduced to one.

It should be noted that the normalization of the above momentum distribution is as in section 4 of ref. [3], that is

$$\frac{1}{(2\pi)^3 A} \int \eta(\vec{k}) d\vec{k} = 1 \quad (27)$$

We also note that expression (26) may be derived directly, and in a simpler way, by using the expression:

$$\eta(k) = \frac{1}{4\pi} \sum_{n,l} \eta_{nl} |\tilde{R}_{nl}(k)|^2 \quad (28)$$

where

$$\tilde{R}_{nl}(k) = \left(\frac{2}{\pi}\right)^{\frac{1}{2}} (-i)^l \int_0^\infty dr r^2 j_l(kr) R_{nl}(r) \quad (29)$$

and $j_l(kr)$ are the spherical Bessel functions of order l , if we take also into account the difference in the normalization, since the $\eta(k)$ given by (28) is normalized to Z . The above expression follows from expressions (7.49) and (7.50) of ref. [3], adjusted to our case. By η_{nl} we denote here the number of nucleons occupying the states with given n and l ($\eta_{nl} = 2(2l + 1)$ for closed shell nuclei).

From expressions (15), (23) and (26), the corresponding state-dependent and state-independent harmonic oscillator results follow immediately for various nuclei. In particular, for the momentum distribution, we find, for the state independent harmonic oscillator results:

a) For 4He

$$\eta_{HO}(k) = 32\pi^{\frac{3}{2}} b^3 e^{-b^2 k^2} \quad (30)$$

b) For 6Li

$$\eta_{HO}(k) = 32\pi^{\frac{3}{2}} b^3 \left(1 + \frac{1}{3} \frac{b^2}{k^2}\right) e^{-b^2 k^2} \quad (31)$$

c) For ${}^{12}C$

$$\eta_{HO}(k) = 32\pi^{\frac{3}{2}} b^3 \left(1 + \frac{2}{3} \frac{b^2}{k^2}\right) e^{-b^2 k^2} \quad (32)$$

d) For ${}^{16}O$

$$\eta_{HO}(k) = 32\pi^{\frac{3}{2}} b^3 \left(1 + 2 \frac{b^2}{k^2}\right) e^{-b^2 k^2} \quad (33)$$

The expression for the state independent harmonic oscillator in the cases of 4He and ${}^{16}O$ are also given in ref. [3].

Another interesting feature of the analytic expression (26) derived is that the asymptotic behaviour of the nucleon momentum distribution for large k is easily obtained and shows a remarkable difference from the corresponding harmonic oscillator expression. By using the well known asymptotic expansion of the confluent hypergeometric function for large x [26,33]:

$${}_1F_1(b, c; x) = \frac{\Gamma(c)}{\Gamma(b)} \frac{e^x}{x^{(c-b)}} \left[1 + \frac{(1-b)(c-b)}{x} + \dots \right] \quad , \quad x > 0 \quad (34)$$

we find that for large values of k the nucleon momentum distribution behaves like:

$$\begin{aligned} \eta(k) &= \frac{\pi^2 2^{4\lambda_0+5} \Gamma^2(\lambda_0+1)}{\Gamma(2\lambda_0 + \frac{1}{2}) \Gamma^2(\frac{1}{2} - \lambda_0)} \frac{1}{b_0^{4\lambda_0+1} k^{4(\lambda_0+1)}} \left[1 + \frac{(\lambda_0+1)(2\lambda_0+1)}{b_0^2 k^2} + \dots \right]^2 \\ &+ (A-4) \frac{\pi^2 2^{4\lambda_1+3} \Gamma^2(\lambda_1 + \frac{3}{2})}{\Gamma(2\lambda_1 + \frac{1}{2}) \Gamma^2(1 - \lambda_1)} \frac{1}{b_1^{4\lambda_1+1} k^{4(\lambda_1+1)}} \left[1 + \frac{\lambda_1(2\lambda_1+3)}{b_1^2 k^2} + \dots \right]^2 \quad (35) \end{aligned}$$

provided that

$$\lambda_0 \neq \frac{1}{2} + n, \quad \lambda_1 \neq 1 + n, \quad n = 0, 1, 2, \dots$$

The dominant term is the first one (see the next section for the values of λ_0 and λ_1) and therefore for sufficiently large values of the momentum k , the momentum distribution tends to zero like an inverse power of k which is determined from the repulsive part of the potential, namely, like $\sim k^{-4(\lambda_0+1)}$. The coefficient of proportionality depends both on the attractive and the repulsive term. We may also note that if both $\lambda_0 = \frac{1}{2} + n$ and $\lambda_1 = 1 + n$, $n = 0, 1, 2, \dots$, the momentum distribution tends to zero for large k very rapidly, namely as a Gaussian or as a power of k times a Gaussian. This situation is however, very unlikely, all the more so since both the above conditions have to be satisfied.

4. Numerical results and discussion.

The results for the nucleon momentum distribution reported in this section have mostly been obtained by using for the values of the potential parameters b and B their best fit values resulting by least squares fitting of the expressions of the elastic charge form factor (see section 3 for the relevant corrections), to the corresponding experimental results, which we know from the elastic electron scattering experiments from light nuclei. Results are reported for 4He , 6Li , ${}^{12}C$ and ${}^{16}O$.

The best fit values for 4He are $b_0 = 0.952 \text{ fm}$, $\lambda_0 = 0.759$. As it is seen from fig. 1 the quality of the fitting is very close to that obtained with the fixed center of mass correction (ref. [29]). The corresponding best fit values

are $b_0 = 1.0575\text{fm}$ and $\lambda_0 = 0.759$. These values are close to those reported in ref. [24]: $b = 1.08\text{fm}$ and $\lambda_0 = 0.74$, which were obtained with a different correction for the finite proton size.

The momentum distribution $\eta(k)$ calculated with the values $b_0 = 0.952\text{fm}$, $\lambda_0 = 0.759$ is shown in fig. 5 (FF dashed line), where the corresponding experimental points are also shown [34]. It should be noted that the values of the momentum distribution in this and the other figures of this section are normalized to unity. It is seen that except for the region of the observed dip, in FF, the calculated values are quite satisfactory. The dotted AS line in fig. 5 (and also in the other figures showing the variation of the momentum distribution with k , for ^6Li , ^{12}C and ^{16}O) depicts the values of $\eta(k)$ obtained by means of expression (35) (neglecting the terms indicated by dots) which was derived with the asymptotic expansion for the Confluent Hypergeometric series and using the parameters from the fitting of the charge form factor. It is seen that for $k > 3.5\text{fm}^{-1}$ the FF line approaches quite closely the AS line.

Relatively improved results in the region of the known experimental values of $\eta(k)$ are obtained, as one should expect, if the parameters are determined by least squares fitting to the experimental values of $\eta(k)$. The values of the parameters are $b_0 = 0.995\text{fm}$ and $\lambda_0 = 0.538$ (see solid line MD of fig. 5).

The FM dotted line in fig. 5 is obtained by least squares fitting to the experimental results of both the form factor and the momentum distribution. In this case, for which $b_0 = 1.078\text{fm}$ and $\lambda_0 = 0.653$, the line differs from the one obtained with the parameters resulting from the fitting of the form factor in the region $k > 2.5\text{fm}^{-1}$, where it lies below the FF dashed line. Finally, the considerable improvement (in comparison to the harmonic oscillator results with the best fit value of the oscillator parameter $b = 1.432\text{fm}$ obtained from the fitting of the form factor), indicated by the solid MD and the FF and FM lines in the region of the larger value of k , (except near the dips in certain cases), is clear.

The results for the charge form factor and the nucleon momentum distribution for ^6Li are given in figures 2 and 6 respectively. The best fit values are in this case $b_0 = 1.452\text{fm}$, $b_1 = 1.868\text{fm}$, $\lambda_0 = 0.560$, $\lambda_1 = 1.022$. It is seen again that the quality of the fitting of the charge form factor is very satisfactory, while with the H.O. model ($b_0 = 1.553\text{fm}$, $b_1 = 1.715\text{fm}$) it is not good for $q^2 \geq 7\text{fm}^{-2}$. In the later case, the average value of the b parameters were used in the Tassie and Barker factor. The nucleon momentum

distribution shows again a pronounced dip and there is considerable increase in the higher values of k , in comparison with the harmonic oscillator results.

In figures 3 and 7 the results for the charge form factor and the nucleon momentum distribution respectively are shown for ^{12}C . The best fit values of $F_{ch}(q)$ are $b_0 = 1.306\text{ fm}$, $b_1 = 1.353\text{ fm}$, $\lambda_0 = 0.647$, $\lambda_1 = 1.406$. The best fit values if state dependence of the potential parameters is not considered are: $b = 1.534\text{ fm}$, $\lambda_0 = 0.573$, $\lambda_1 = 1.03$. The results with the harmonic oscillator model have been obtained with the best fit value $b = 1.626\text{ fm}$. It is seen from fig. 3 that the fitting of the charge factor is very good with the present model if state dependence of the parameters is considered. With the simple H.O. model the fitting is also quite satisfactory, though worse in comparison with this model as one should expect. The difference of the results obtained with the two models is much more pronounced as far as the momentum distribution is concerned. In this case the harmonic oscillator fails completely to reproduce the data for large k while with the present model the situation is considerably improved, although there is still disagreement in the region of the larger values of k ($k \geq 1.7\text{ fm}^{-1}$). Use of the state independent best fit values gives worse results for the larger k values. The other interesting observation one can make is that if the parameters are determined by least squares fitting of the theoretical expression for the nucleon momentum distribution to the corresponding experimental results, a very good fit on the whole is obtained (except for some deviations, mainly at small k). Moreover, the dip (around $k = 2\text{ fm}^{-1}$) almost disappears in this case (see MD solid line of fig. 7). The corresponding best fit values are: $b_0 = 0.789\text{ fm}$, $b_1 = 1.079\text{ fm}$, $\lambda_0 = 1.518$, $\lambda_1 = 3.155$.

The results for ^{16}O are displayed in figures 4 and 8 for the charge form factor and the nucleon momentum distribution, respectively. The best fit values of $F_{ch}(q)$ are: $b_0 = 1.18\text{ fm}$, $b_1 = 1.40\text{ fm}$, $\lambda_0 = 0.798$, $\lambda_1 = 1.634$, while for the state independent best fit values we obtain $b = 1.727\text{ fm}$, $\lambda_0 = 0.551$, $\lambda_1 = 1.02$. For the harmonic oscillator model $b = 1.762\text{ fm}$. It is seen that the fit of F_{ch} is good except for the large values of q , where there are deviations, which are more pronounced in the state independent case. It is, however, better than the one obtained with the harmonic oscillator model. The behaviour of the nucleon momentum distribution is rather similar to that of ^{12}C .

In conclusion, the detailed analysis described in this paper for light nuclei indicates that although the elastic charge form factor and the nucleon momentum distribution cannot be fitted simultaneously with a single particle potential model, as it is well known, considerable improvement can be achieved in general if a short range repulsion is included in this potential.

The authors would like to thank Prof. A. Antonov and Drs S. Massen and M. Stoitsov for useful discussions and suggestions.

References

- [1] S.Frullani and J.Mougey, Adv. Nucl. Phys. Vol.14 (1985) ed. by J.Negele and E.Vogt.
- [2] B.Frois and C.N.Papanicolas, Ann. Rev. Nucl. Part. Sci. 37 (1987) 133
- [3] A.N.Antonov, P.E.Hodgson and J.Zh.Petkov, Nucleon momentum and density distributions, in nuclei, Clarendon press, Oxford 1988
- [4] "Momentum distributions", Argonne National Laboratory, October 1988, ed. by R.N.Silver and P.E.Sokol, Plenum press, N.Y, (1989)
- [5] P.K.A. de Witt Huberts, J. Phys. G Nucl. Part. Phys. 16 (1990) 507.
- [6] S.Stringari, M.Traini and O.Bohigas Nucl. Phys. A516 (1990) 33
- [7] J.G.Jabolitzki and W.Ey, Phys. Lett. 76B (1987) 527
- [8] J.W. Van Orden, W.Truex and M.K.Banerjee Phys. Rev C21 (1980) 2628
- [9] A.N.Antonov, V.A.Nikolaev and I.Zh.Petkov Z. Phys. A297, (1980) 257
- [10] A.N.Antonov, I.Zh.Petkov, Nuovo Cimento A94 (1986) 68;
A.N.Antonov, I.Zh.Petkov, P.E.Hodgson, Bulg. Journal of Physics 13 (1986) 110
- [11] M.Dal Ri, S.Stringari and O.Bohigas, Nucl. Phys. A376 (1982) 81
- [12] Y.Akaishi, Nucl. Phys. A416 (1984) 409
- [13] R.Schiavilla, V.R.Pandharipande and R.B.Wiringa Nucl. Phys. A449 (1986) 219
- [14] M.Casas, J.Martorell, E.Moya de Guerra and T.Treiner Nucl. Phys. A473 (1987) 429
- [15] H.Krivine, Nucl. Phys. A457 (1986) 125

- [16] O.Benhar, C.Ciofi degli Atti, S.Liuti and G.Salmé, Phys. Lett. 177B (1986) 135 ; C.Cioffi degli Atti, E.Pace and G.Salmé, Phys. Rev. C36 (1987) 1208 ; C.Cioffi degli Atti, Few body systems Suppl. 2 (1987) 140
- [17] F.Dellagiacoma, G.Orlandini and M.Traini, Nucl. Phys. A393 (1983) 95
- [18] M.Traini and G.Orlandini, Z.Phys. A321 (1985) 479
- [19] M.Jaminon, C.Mahaux and Ngo, Nucl. Phys. A452 (1986) 445
- [20] M.L.Ristig, P.M.Lam and A.Lejeune, Phys. Let. 93B (1980) 240; M.Modarres, Europhys. Letters 3 (1987) 1083
- [21] M.F.Flynn, J.W.Clark, R.M.Panoff, O.Bohigas and S.Stringari, Nucl. Phys. A427 (1984) 253
- [22] S.Fantoni and V.R.Pandaripande, Nucl. Phys. A427 (1984) 473
- [23] E. Moya de Guerra, P.Sarriguren, J.A.Caballero, M.Casas, D.W.L.Sprung, Nucl. Phys. A529 (1991) 68; J.A.Caballero and E.Moya de Guerra, Nucl. Phys. A509 (1990) 117.
- [24] M.E.Grypeos and K.N.Ypsilantis, J.Phys. G Nucl. and Part. Phys. 15 (1989) 1397
- [25] F.Constantineskou and E.Magyari, Problems in Quantum Mechanics Pergamon Press, Oxford 1976
- [26] M.Abramowitz, I.A.Segun, Handbook of Mathematical Functions, Dover Publications, Inc., New York 1968
- [27] L.R.B.Elton, Nuclear Sizes, Oxford Univ. Press, 1961
- [28] L.J.Tassie and F.C.Barker, Phys. Rev. 111 (1958) 940
- [29] S.Radhakant, S.Khadkikar, B.Banerjee, Nucl. Phys. A142 (1970) 81
- [30] H.Chandra and G.Sauer, Phys. Rev C13 (1976) 245
- [31] C.Daskaloyannis, M.Grypeos and H.Nassena, Phys. Rev. C26 (1982) 702

- [32] H.Buchholz, "The confluent Hypergeometric function", Springer-Verlag, Berlin 1969
- [33] G.Arken, Mathematical Methods for Physicists, Second Ed., Acad. Press, New York-London (1970)
- [34] A.Antonov and P.E. Hodgson and J. Zh. Petkov, Nucleon correlations in nuclei, Springer Verlag, Berlin 1993 and references cited there.

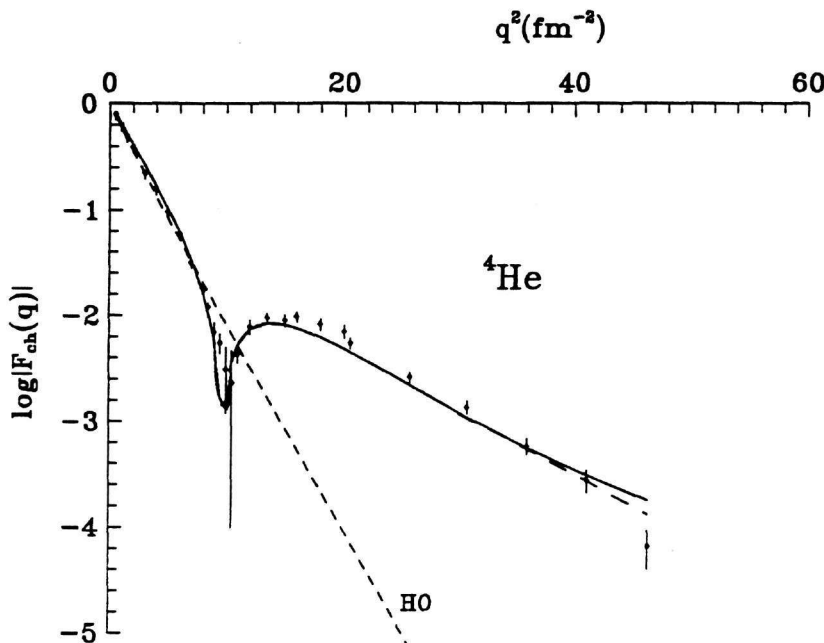


Fig. 1. The charge form factor of ${}^4\text{He}$ obtained with the present approach using the reduced mass (full line) and "fixed center of mass correction" (dashed line). The HO dashed line is the harmonic oscillator model with the best fit value $b=1.432$ fm (obtained with the Tassie and Barker factor for the center of mass correction).

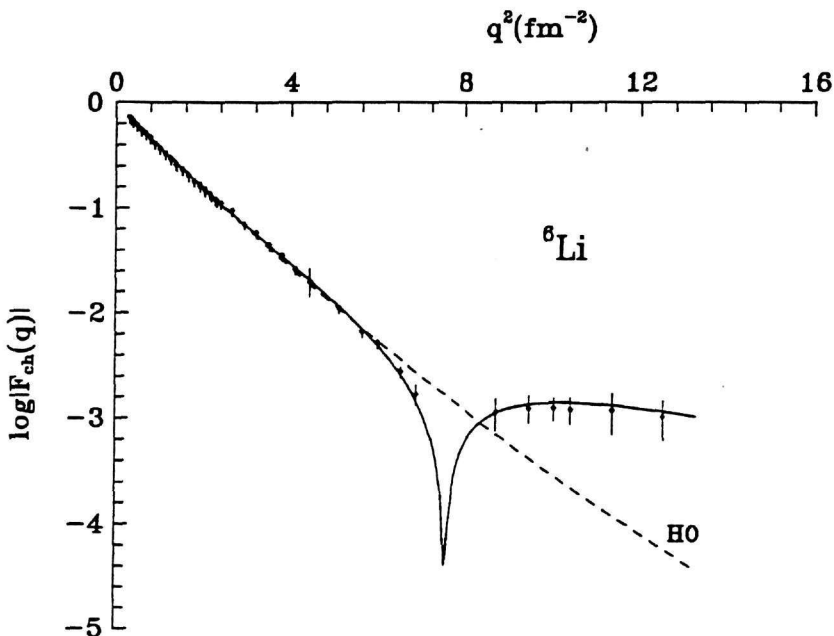


Fig. 2. The charge form factor of ${}^6\text{Li}$ obtained with the present approach (full line) and the one with the harmonic oscillator model (HO dashed line) with $b_0=1.553$ fm and $b_1=1.715$ fm.

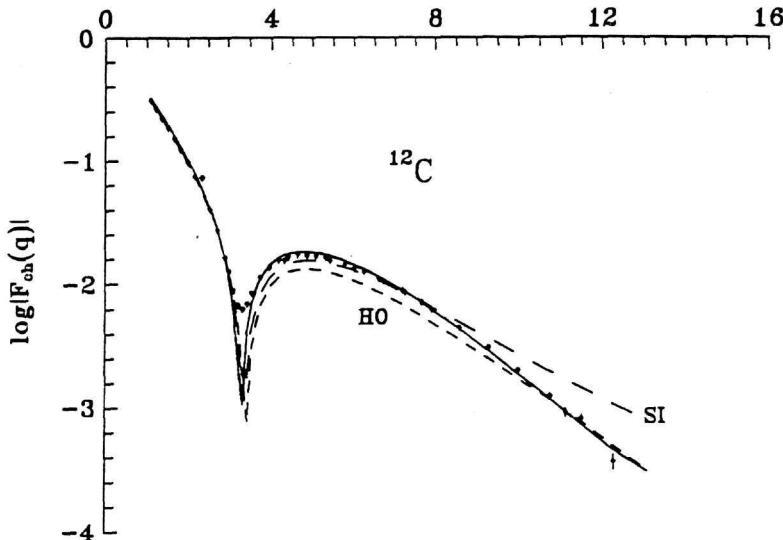


Fig. 3. The charge form factor of ^{12}C obtained with the present approach (full line) and the one with the harmonic oscillator model (HO dashed line) with $b=1.626$ fm. The SI dashed line is the state independent case with $\lambda_0=0.573$, $\lambda_1=1.03$ and $b=1.534$ fm.

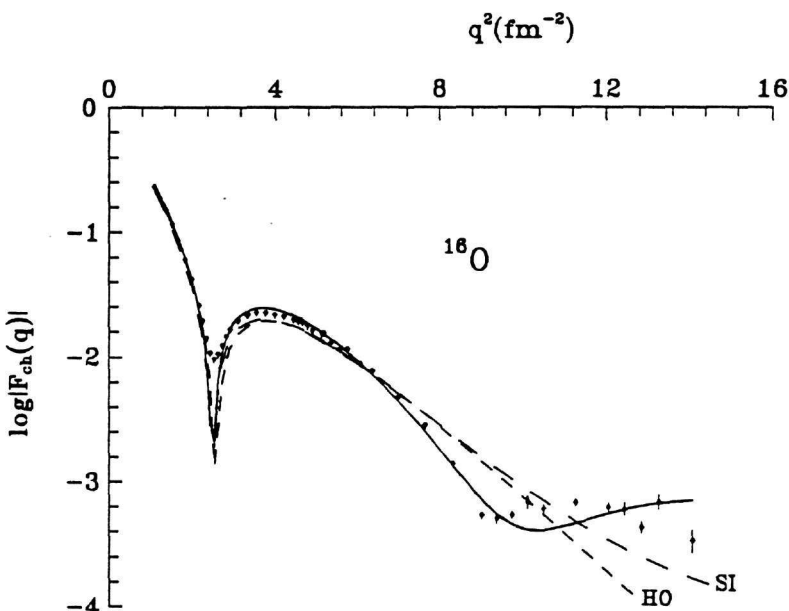


Fig. 4. The charge form factor of ^{16}O obtained with the present approach (full line) and the one with the harmonic oscillator model (HO dashed line) with $b=1.762$. The SI dashed line is the state independent case with $\lambda_0=0.551$, $\lambda_1=1.02$ and $b=1.727$ fm.

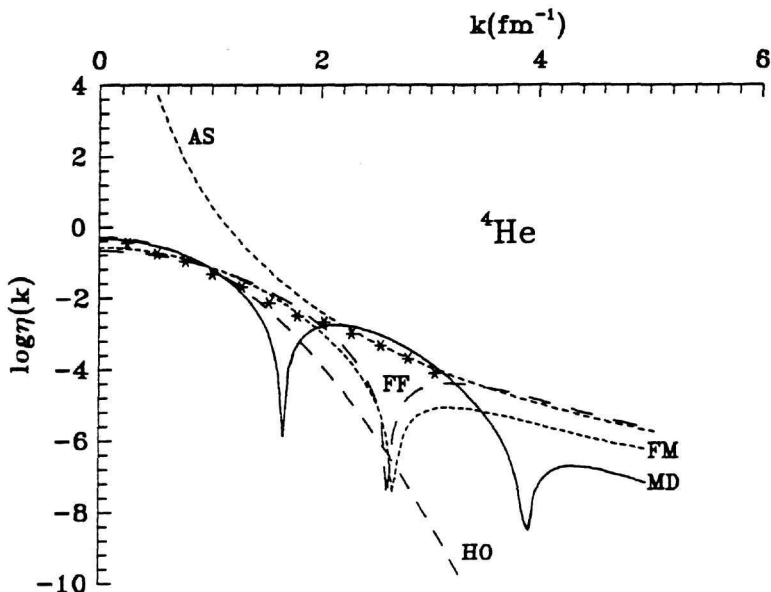


Fig. 5. The nucleon momentum distribution of ${}^4\text{He}$. The FM line is drawn using the parameters determined from the fitting of the form factor and the momentum distribution. The FF line is drawn using the parameters from the fitting of the form factor. The MD line is the momentum distribution obtained with the present approach by fitting to the experimental $\eta(k)$ values. The HO line is the harmonic oscillator momentum distribution and the AS line is the asymptotic behaviour of the momentum distribution FF.

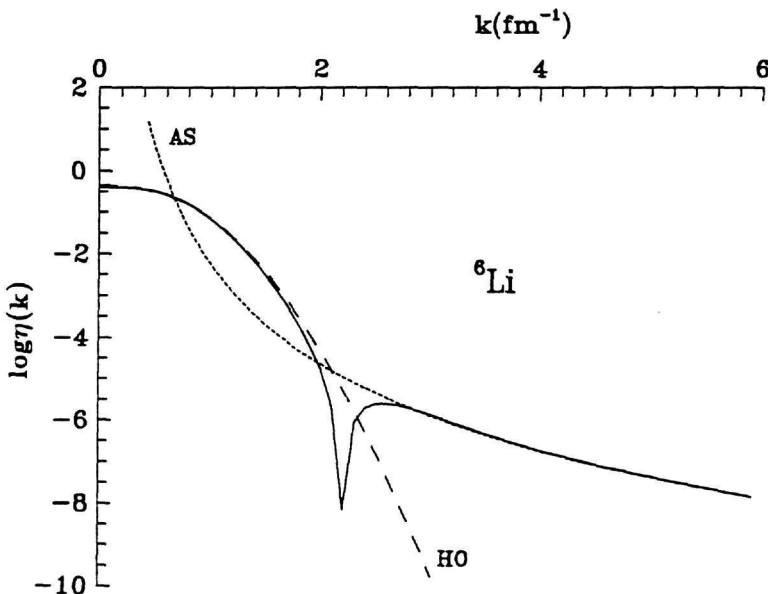


Fig. 6. The nucleon momentum distribution of ${}^6\text{Li}$ with the present approach using the parameters from the fitting of the form factor (full line) and with the harmonic oscillator model (dashed line). The AS dotted line is the asymptotic behaviour of the momentum distribution.

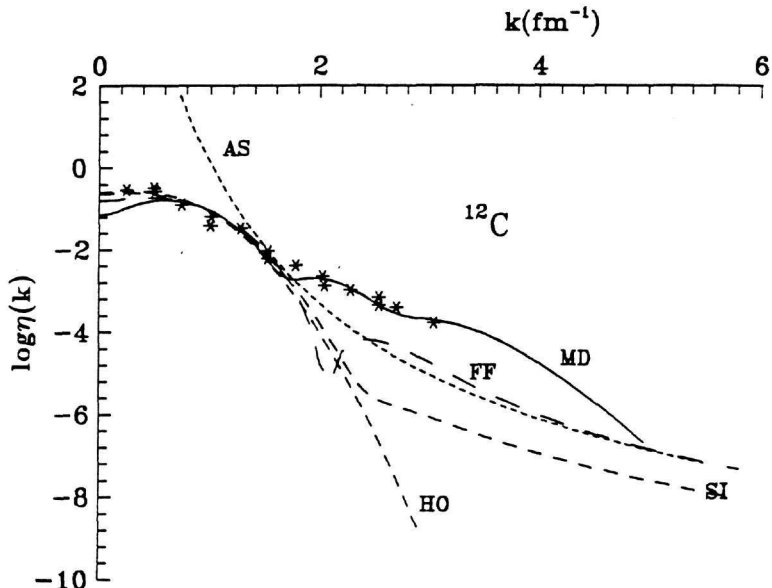


Fig. 7. The nucleon momentum distribution of ^{12}C obtained with the present approach by fitting to the experimental $\eta(k)$ values (MD full line), using the parameters determined from the fitting of the form factor (FF dashed line) and its asymptotic behaviour (AS dotted line). The HO dashed line is the harmonic oscillator nucleon momentum distribution. The SI dashed line is the nucleon momentum distribution with the state independent parameters in the fitting of the form factor.

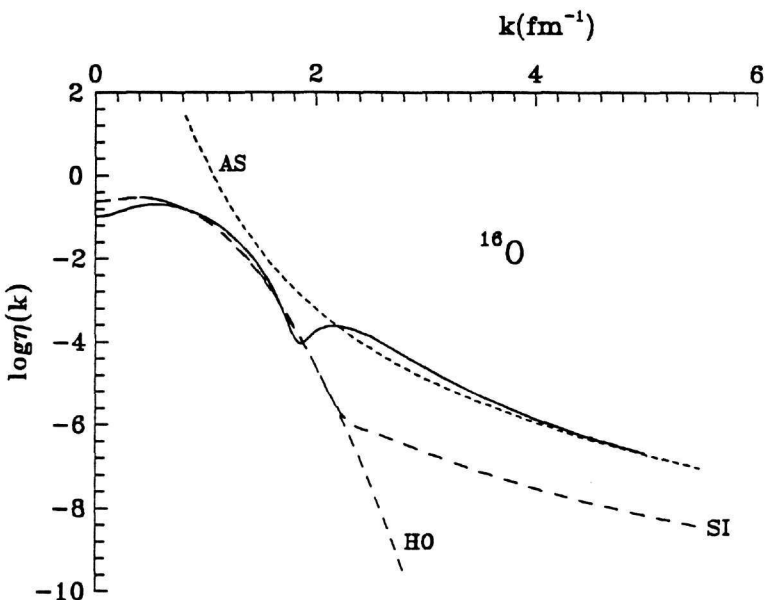


Fig. 8. The nucleon momentum distribution of ^{16}O with the present approach using the parameters from the fitting of the form factor (full line) and with the harmonic oscillator model (HO dashed line). The AS dotted line is the asymptotic behaviour of the nucleon momentum distribution. The SI dashed line is the nucleon momentum distribution with the state independent parameters in the fitting of the form factor.